

# Study on the Nonlinear Responses of Concentrically Braced Steel Frame Structure under Diverse Intensities of Earthquake

**Z. G. Xu, X. Y. Cheng & C. Z. Xiao**

*China Academy of Building Research, China*



## SUMMARY:

The present study investigates the nonlinear responses of one 7-story, 92 meters high concentrically braced steel frame structure under multiple earthquake intensity ground motions with inelastic time-history analysis. The yield mechanism and the failure pattern of the concentrically braced steel frame structure were revealed and the relationships between structural global deformations (story displacement and inter-story drift) and the peak acceleration value of earthquake motions were also studied. It is shown that the concentric braces could be buckled due to self-inertia effect during strong ground motions although initial imperfections are not introduced. Results indicate that the buckling and post-buckling characteristics of concentric braces have significant influences on the global deformations, yield mechanism and failure pattern of the structure. This paper also discussed the importance of brace member in the structure and proposed some suggestions for the seismic design and collapse prevention.

*Keywords: Nonlinear history analysis, yield mechanism, failure mode*

## 1. INTRODUCTIONS

Concentrically braced steel frame structure is one popular type of structural systems for industrial plant buildings. In cement plant buildings, the concentrically braced steel frame structure is usually used to hold the key equipments such as calciners in cement production lines. During 5.12 WENCHUAN EARTHQUAKE OF 2008, this type structure in a number of cement plants were collapsed and directly stunted the rehabilitation works in disaster zones. One important lesson from the catastrophe is the seismic performance of the structure under intensive earthquakes has important role to guarantee the reliability of the structure, equipments safety, and even the whole cement production lines failure-free operation during the special period.

However, from the current published literatures, a little has been reported for the seismic analysis of this type structure, the nonlinear response and the seismic performance under the strong earthquake intensity ground motions is less reported even. In this paper, one real concentrically braced steel frame structure, a key industrial building for holding calciners in the cement production lines (seen as Fig.1), was selected as research subject and a series nonlinear time history analyses were carried out to investigate the seismic responses under divers intensity earthquakes with artificial ground motion records. These results and their discussion focus on: 1) the influence of diverse earthquake intensities on the structural nonlinear responses of displacements, drifts and yielding mechanisms; 2) the failure modes of the structure under intensive earthquakes; 3) the influence of key structural members' failure mechanisms on the structural seismic performance under intensive earthquakes and design recommendations



**Figure 1.1** Picture of the braced steel frame structure

## 2. RESEARCH OBJECTS AND METHODS

### 2.1. Structure Overview

The structural plan and elevations is shown as Fig.2.1. Reinforced concrete frame structure is used under the elevation of 7.500m, the surrounding columns square sections are 1500mmx1500mm and 1600mmx1600mm, the centrals is 1000mmx1000mm and the concrete grade is C40. The concentrically braced steel frame structure with concrete filled steel tube (abbreviated as CFT) columns are used above the elevation of 7.500m, the diameters of corner CFT columns are 850mm and the centrals is  $\Phi 900$ mm. The hot-rolled seamless steel pipes are used as the brace between columns. The welded I-section steel is used for beams. The slab of first floor is reinforced concrete (C30 grade) slab with 120mm thick and the others are 6mm thick steel plate. The steel grade of CFT columns, the concentric braces and the beams which support the equipments is Q345-B. The steel grade of other steel members is Q235-B. According to the Chinese Code for Seismic Design of Buildings (GB50011-2001) and the Chinese Standard for Classification of Seismic Protection of Building Constructions (GB50223-95), the seismic precautionary intensity is VII grade, the seismic fortification category for structure is B grade, the classification of design earthquake is 1st group, the site classification is II class, the design characteristic period of ground motion is 0.35s.

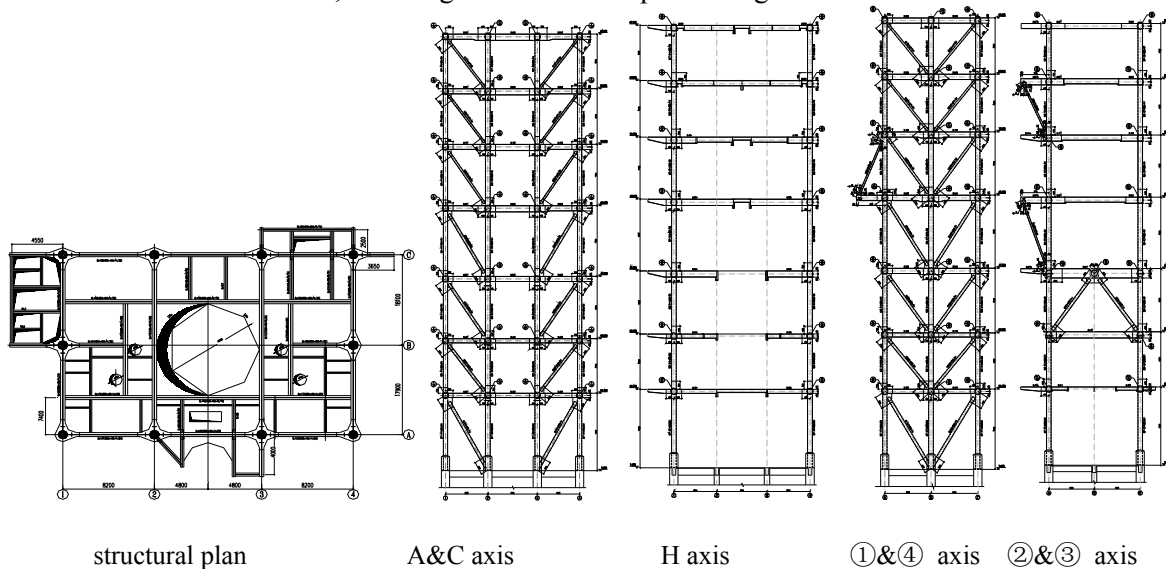


**Figure 2.1** Plan and Elevations of the structure

### 2.2. The Descriptions of Analysis Method

In this study, the nonlinear time history analyses were conducted with Abaqus, one well-known finite

element analysis software. The selected constitutive law for steel material is the bilinear kinematic hardening model (shown in Fig. 2.2). In this model, there is no stiffness degradation during the loading and unloading cycles. The yield strength of the different grade steel material is determined according to Chinese codes and the post yield stiffness slope is 2.5% times elastic modulus. The selected constitutive law for concrete is uniaxial cyclic law with monotonic envelope governed by the recommended curve in the Chinese Code for Design of Concrete Structure (GB 50010-2001). The implemented cyclic behavior is characterized by linear unloading–reloading branches with progressively degrading stiffness. After each unloading/reloading sequence, the monotonic envelope is reached again when the absolute value of the largest compressive strain attained so far is surpassed. The concrete in tension follows the same loading/unloading/reloading rules as in compression with the same initial stiffness and appropriate values for the other parameters. A more detailed description of the monotonic and cyclic behavior is given in Xu et al. (2011). A typical cyclic response of the concrete material model adopted in this study is shown in Fig. 2.3.

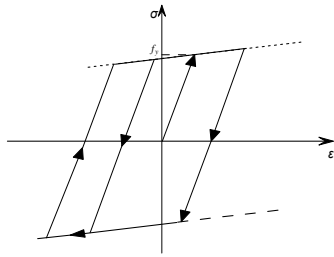


**Figure 2.2** Bilinear kinematic hardening model for steel

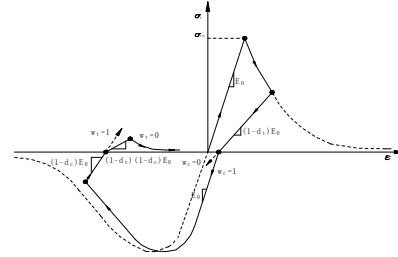


**Figure 2.3** Plastic damage model for concrete

It should be noted that the peak compression/tension strengths of concrete material adopted the standard values defined by the Chinese code and the confinement effects caused by stirrups and steel tubes were not considered.

In the structural finite element model, different finite element formulations for structural members were adopted based on the deform behavior: quadrilateral or triangular shell element is used for representing the slab and three-node space beam-column element based on fibre model is used for representing column, beam and brace. In the calculation process, the gravity analysis is performed firstly, and then the dynamic inelastic analysis continued on that basis. The adopted time integration scheme is the explicit central different method. The structural damping properties were represented by proportional to the element masses and the damping ratio is taken 5% for concrete material, 3% for steel material to derive corresponding material damping factor respectively.

### 2.3. The Descriptions of Analysis Cases

In order to keep the consistent with the basic idea of structure seismic design in Chinese codes and the avoid analysis diversities because of the ground motion uncertainty, the artificial records (duration is 20s) were selected as input, whose spectrum characteristics are more consistent with the design response spectrum defined in Chinese code. And one direction inputting strategy in analysis was adopted for highlighting the major influence factors toward the seismic performance. The peak accelerations of ground motions (abbreviated as "PGA") were chosen as 55gal, 110gal, 150gal, 200gal, 310gal, 400gal and 510gal respectively. The nonlinear analysis cases are total 14 and cover the seismic intensities for VII grade to VIII grade corresponding to the Chinese Code for Seismic Design of Buildings for site classification II. The artificial earthquake wave and its spectral curve are shown in Fig. 2.4.

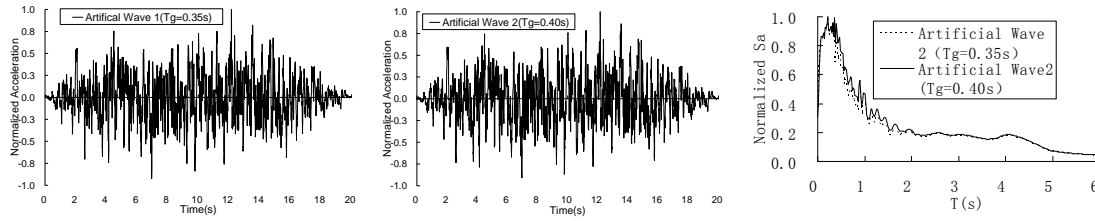


Figure 2.4 Artificial waves and spectra

### 3. ANALYSIS RESULTS

#### 3.1. Vibration Analysis

The natural vibration periods and the vibration characteristics are listed in table 3.1. It can be seen that the natural vibration shape is fine, the ratio between the first torsion period and the first translational period is 0.54, and although the number of the column in the y direction is less than the x direction, the lateral stiffness of y direction is still larger than that of x direction because of stiffer braces.

Table 3.1 The periods and modal characteristics of the structure

Mode Number	1	2	3	4	5	6
period(s)	2.34	1.93	1.26	0.72	0.66	0.44
Vibration characteristic	x-translation	y-translation	z-torsion	x-translation	y-translation	z-torsion

Briefly, the dynamic responses of structure are presented and discussed with the envelope values below.

#### 3.2. Floor Displacements

The distribution curve of the maximum floor displacements under the various PGA is shown in Fig. 3.2. It can be seen that the maximum floor displacement distribution curve are similar when PGA is less than 310gal. As the PGA increased, the maximal floor displacements of third floor and above under x direction input and those of fifth floor and above under y direction input increased greatly. In the case of PGA 510gal, the floor displacement distribution curve had apparent anti-s shape. The curves of maximum displacements of each floor under diverse PGA are shown in Fig. 3.3. It can be seen that there are some differences in the maximum floor displacement between two input directions: In the x direction input, the maximum floor displacements of the first and second floor increased linearly when PGA is less than 310 gal and the maximum displacement curves of other floors bent after PGA lager than 200 gal and increased slowly. In the y direction input, the maximum floor displacement from the first to fifth story increased linearly when PGA is less than 310 gal and bent apparently after PGA is lager than 310gal. Above the 400gal, it is more apparent at the sixth, the seventh and the eighth floor.

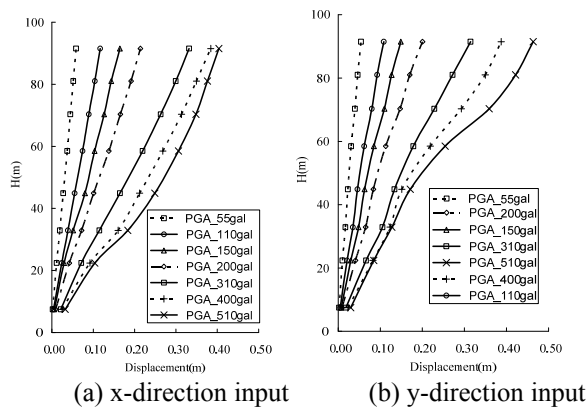


Figure 3.3 Maximum floor displacements vs. PGAs

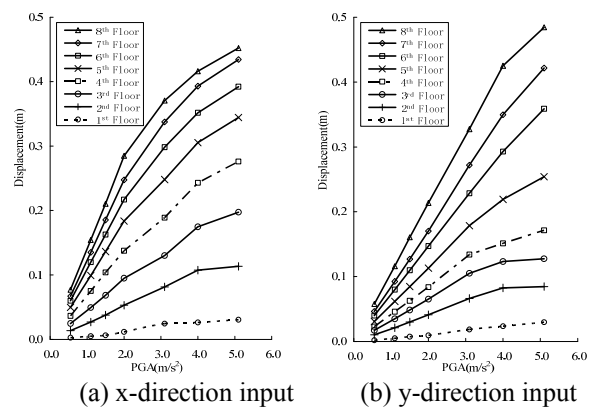
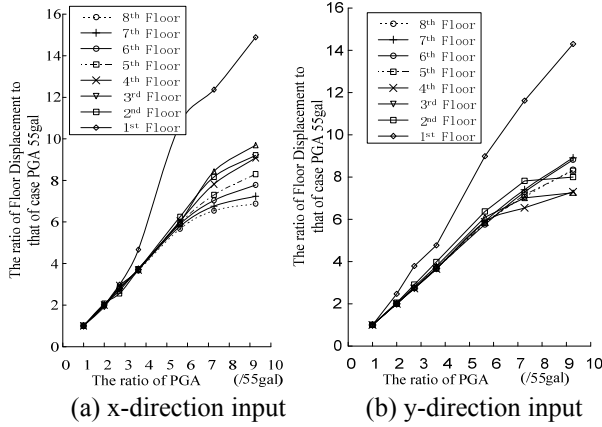
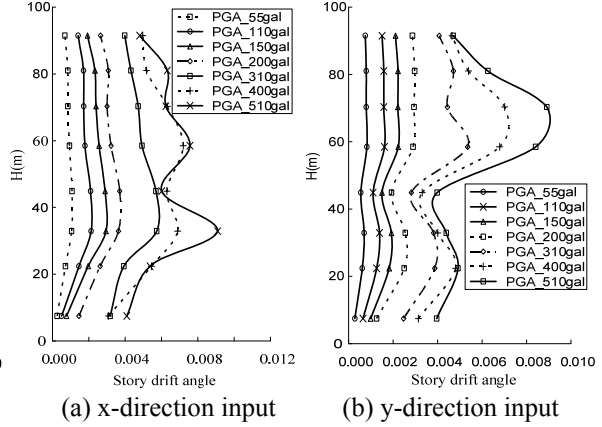


Figure 3.4 Maximum floor displacements vs. PGAs

The ratio of the maximum floor displacement to that of case PGA 55gal is shown in Fig.3.5. It can be seen that the amplificatory ratio of the first floor is larger than the others in both x and y direction inputs and that of PGA as well. After the PGA was larger than 310gal, the amplification of the maximum floor displacement was reduced evidently and less than the times of the PGA increasing relatively except the first floor.



**Figure 3.5** The amplifications of maximum floor displacement



**Figure 3.6** The distributions of maximum inter-story drift ratio

### 3.3. Story Drifts

The distribution curves of the maximum interstory drift ratio are shown in Fig. 3.6 under the various PGAs. It can be seen that the curve distributions along the floor height are similar when the PGA is less than 200gal. As the PGA increased, the maximum interstory drift ratio of 3rd story and that of 5th were increased under x and y direction inputs respectively. For x direction input, the maximum interstory drift ratios of the 3rd, 4th and 5th stories were significantly increased after PGA larger than 400gal due to the plasticity formation in structure. However, the maximum interstory drift ratio distributions were not changed obviously for y direction input. For the case of PGA 510gal, the maximum interstory drift ratio is 1/128(the 3rd story) and 1/118(the 6th story) under x and y direction input respectively, which is smaller than 1/50 given by Chinese codes. The distribution curves of the maximum interstory drift ratios under various PGA are shown in Fig. 3.7. Under the x direction input, it can be seen that the maximum interstory drift ratios are increased linearly when PGA was less than 400gal. While the maximum interstory drift ratios of 1st and 3rd story were increased significantly and those of the other stories were increased slowly even reduced after PGA was over 400gal. Under the y direction input, it can be seen that the maximum interstory drift ratios were increased linearly when PGA was less than 310gal. While the maximum drift angles of the 1st and 6th story were increased significantly after PGA was over 310gal.

The ratio of the maximum interstory drift ratio to that of the case PGA 55gal is shown in Fig. 3.8. It can be seen that the amplificatory ratio of the first story is larger than the others in both x and y direction inputs and that of PGA as well. In addition, After PGA is larger than 400gal, the amplificatory ratios of the maximum interstory drift ratios kept constant as the PGA increasing except the 1st, 5th and 7th story under x direction input. The amplificatory ratios of the maximum interstory drift ratios kept constant as the PGA increasing except the 1st, 5th and 6th story under y direction input.

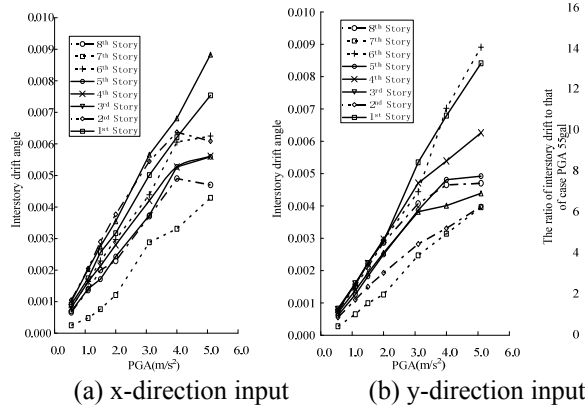


**Figure 3.7** The amplification of maximum interstory drift ratio

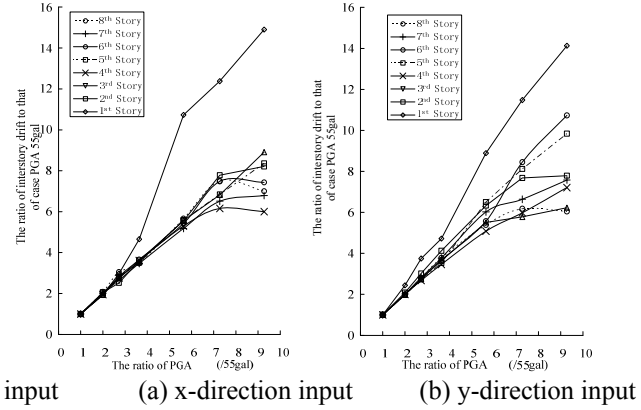


**Figure 3.8** The amplification of maximum interstory drift ratio

## 4. STRUCTURAL YIELD MECHANISM

For x and y direction input with PGA 55gal, the structure was elastic. Some steel beams at the 2nd, 4th and 6th floor were sequentially yielded when PGA was 110gal, 150gal and 200gal. Some plasticity began to arise at some concentric braces in 5th story when PGA reached 310gal. In cases of PGA 400gal and 510gal, serious plasticity concentrated at the beams at 2nd, 4th and 6th floor, the braces in 5th to 8th stories and the columns in 1st story. In summary, the structural progressive yield mechanism is some beams, then the braces in 5th and 6th story and the columns in 1st story at last. Fig. 4.1 shows the typical plastic strain distributions under x direction inputs with divers PGAs.

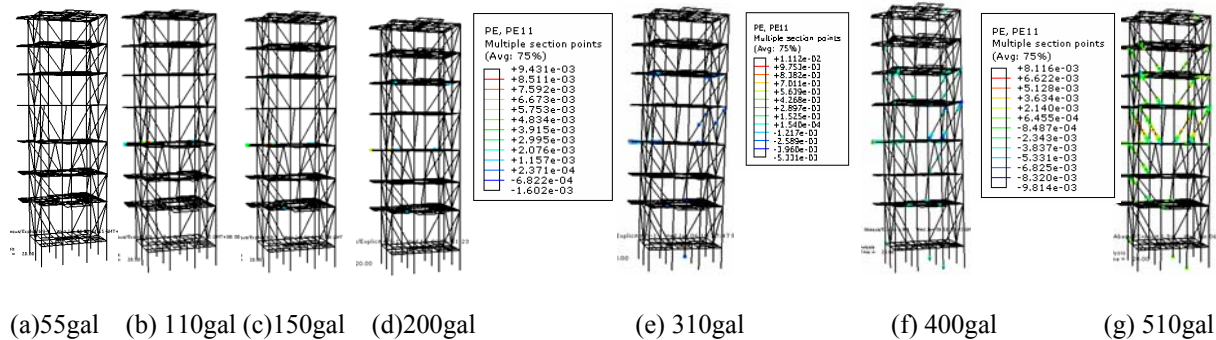


**Figure 4.1** Structure plastic strain distributions under x direction inputs with different PGA

## 5. FAILURE MODES

To investigate structural responses under intensive earthquakes, especially the structural failure modes are of importance for aseismic engineering all the time. In a sense, to grasp the potential failure modes of structure means to seize the soul of seismic design for structure.

### 5.1. Columns

The structural columns in the first and fifth story at the intersection of axis A and axis 1 are selected (shown as Fig. 2.1). The axial forces and bending moments in each analysis were extracted and compared with the corresponding values of yield and limit state.

As Fig.5.1 and Fig.5.2 shows, the columns' internal forces resultant points which are combined by maximal and minimal axial force vs. corresponding moment and maximal moment vs. corresponding axial force in each analysis, are plotted with the section axial force and moment interaction (abbreviated as N-M interaction) curves. Here the yield  $N_y$ - $M_y$  interaction curve and the limit  $N_u$ - $M_u$  interaction curve were both derived with plane section assumption but using design and standard

material strength respectively. It can be seen that the internal forces of the selected columns increased as the PGA increased and more significant for the column in 1st story. After the PGA exceeded 310gal, each selected column's moment increased more significantly than the axial force did and some internal force resultant points of the first and fifth story even beyond the yield state and close to the limit state.

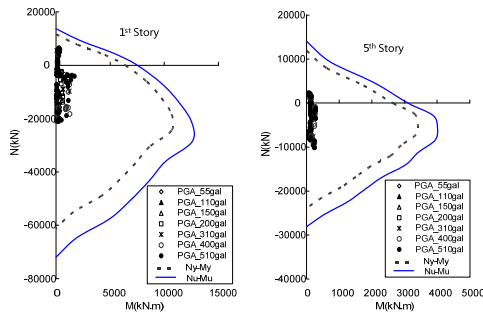


**Figure 5.1** N-M checking for corner columns under x direction inputs

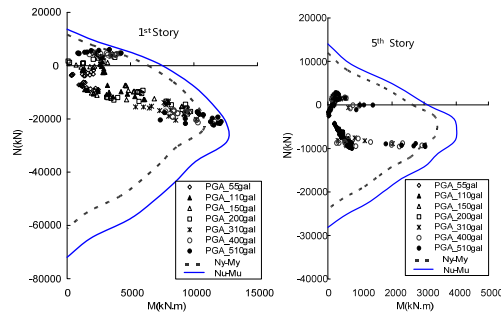


**Fig 5.2** N-M checking for corner columns under y direction inputs

In addition, it is worthy to note that the structural columns keep in the compression state in the smaller PGA cases because of gravity. But as the PGA increased, the axial force of column increased and gradually turned to tension range. The failure of the first story columns was caused by tension and bending in the case of PGA 510gal, y direction input.

## 5.2. Braces

For this structure, the diagonal braces are very important structural members. To study their failure modes in the cases of PGA 310gal and PGA 510gal, the relationships of axial forces vs. axial deformations of the selected braces in fifth story (shown as Fig. 5.3) are shown as Fig.5.3. The sections of selected braces are  $\phi 500 \times 10$  along x direction and  $\phi 500 \times 12$  along y direction respectively.

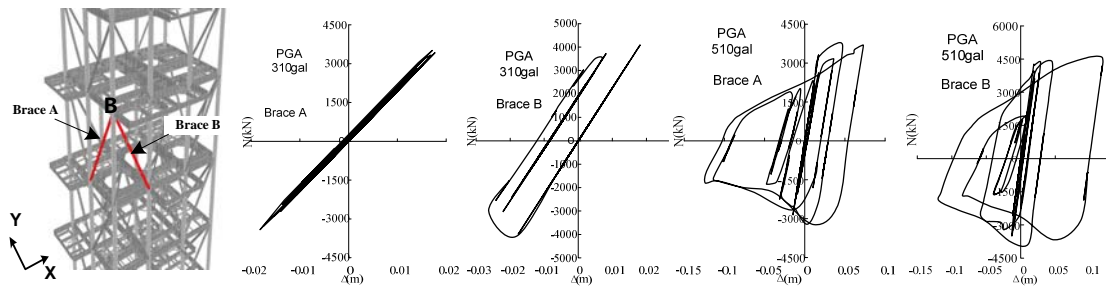


**Figure 5.3** Axial force vs. deformation hysteretic curves of braces under PGA 310gal and PGA 510gal

From Fig.5.3, it can be seen that the selected brace along x direction is basically elastic in the cases of PGA 310gal. But for the brace along y direction, the axial forces are reducing gradually as axial deformations increasing in compression, so-called buckling state. By checking the maximum axial force and evaluated theoretical section capacity ( $A_s \times f_y = 18397 \times 235 = 4323.3 \text{ kN}$ ), the ratio is only 0.94. The compression plastic deformation is about 10mm finally. In the case of PGA 510gal, the selected braces showed both tension yielding and compression buckling phenomenon significantly. It should be noted that the initial imperfections for all members including braces were not introduced in these analysis, the main reasons for the compression buckling of the braces would be their larger length (about 16m) and the strong coupling effect of axial force and the lateral displacements caused by their own inertia acting during the earthquakes. And the coupling effect would increase much more as the PGA increasing.

## 5. CONCLUSIONS

In this paper, a series nonlinear time history analyses were carried out and investigated the nonlinear responses of one concentrically braced steel frame structure under diverse intensity earthquakes. The principles of structural deformation with the peak ground acceleration and structure yield mechanisms under diverse intensity earthquakes were presented. The failure modes were also revealed by involving the responses of columns and braces. From this study, some valuable conclusions for this type structure aseismic design can be drawn:

- 1) The structure deformation pattern will be affected by the structural yield mechanism apparently. The story displacement and drift will increase greatly due to the yielding of the lateral resistance members (especially the braces) in the story under intensive earthquake.
- 2) According to the structural yield mechanism and the failure mode, it can be seen that the bearing state of structural member will be changed to adverse conditions under intensive earthquake. Moreover, the adverse conditions usually are ignored in the design phase due to small earthquake effect. For example, in this study the bearing states of CFT columns will be turned to tension-bending from compression-bending in initial design state, which is very harmful.
- 3) Braces play very important role for concentrically braced frame structure. They provide great parts of lateral stiffness when elastic. But their yielding and buckling under intensive earthquake will cause unexpected harm to structural deformation and other members bearing states.
- 4) In this study, braces shows obvious buckling failure mode due to the coupling of axial forces and their self inertia effects though no initial imperfections were introduced. This phenomenon reminds our structural engineers of the inertia adverse effects for buckling design.

## REFERENCES

- Xu, Z.G. et al. (2009). The Research of the Seismic Responses about the Pre-heater Tower in NSP Cements Production Lines, Institute of Building Structure, China Academy of Building Research, Beijing China
- Committees of National Standard of the People's Republic of China (2001), Code for Design of Concrete Structures (GB 50010-2001) (in Chinese). China Architecture & Building Press, Beijing,. China
- Committees of National Standard of the People's Republic of China (2001), Code for Seismic Design of Buildings (GB 50011-2002) (in Chinese). China Architecture & Building Press, Beijing,. China
- Xu, Z.G. Xiao, C.Z. Ren C.C. (2011). Edifications on the aseismic design of high-rise building from structure elastoplastic analysis. *Building Structure* **41:11**, 41-46.